Chapter 3

Study of the DEP_C-PH double-domain protein

The characterisation of single domains is an invaluable first step to understand the function of a protein. Yet, domains are rarely autonomous entities: their function is often fine-tuned in the context of their biological environment. Intermolecular as well as intramolecular interactions provide the key to the biological function and regulation of multi-domain proteins.

As for pleckstrin, all three single domain (N-PH, DEP and C-PH) structures are now available (cf. chapter 2) and interactions of both N-PH and C-PH with phosphoinositide ligands have been studied (Harlan et al., 1994; Harlan et al., 1995, chapter 2). Conversely, the quaternary arrangement of the domains of pleckstrin is not known and intramolecular interactions are uncharacterised. In preliminary studies, no direct interaction between separately expressed single domains of pleckstrin was observed (G. Stier, M. Macias, unpublished results). However, this does not mean that they do not interact when they are part of the same polypeptide chain (*in cis*) and when the inter-domain linker present. In order to study the linker sequences and the interaction between vicinal domains *in cis*, double-domain constructs (N-PH_DEP and DEP_C-PH) of pleckstrin are generated.

The backbone resonances of N-PH_DEP have already been assigned and compared to single N-PH and DEP (B. Simon, unpublished results). These data show an interaction between N-PH and DEP domain. In the current chapter, the DEP_C-PH double-domain construct is studied by NMR and biochemical methods and its properties are compared to the single DEP and C-PH domains.

3.1 Results

3.1.1 Construct definition and sample preparation

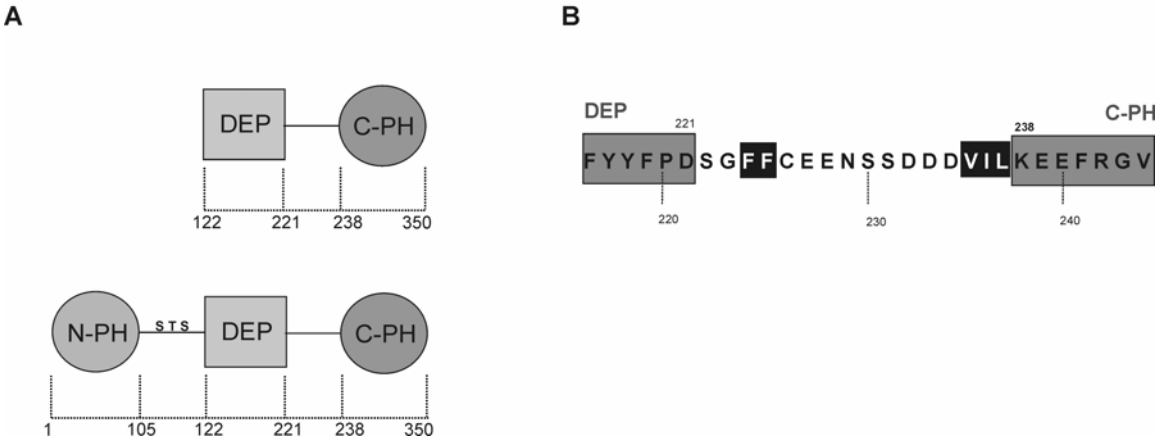

Figure 3.1: The DEP_C-PH construct. A*: schematic representation of the DEP_C-PH. For comparison, the full-length molecule is shown below.* ***B****: The inter-domain linker sequence between DEP and C-PH. Hydrophobic residues in the linker are in white on black background.*

The boundaries of the DEP_C-PH are chosen based on the known structures of the DEP and C-PH domains. The construct consists of amino acids 122-350, i.e. from the N-terminus of the DEP domain to the C-terminus of C-PH (which is also the native C-terminus of the pleckstrin protein, Fig 3.1A). Fig. 3.1B shows the inter-domain linker sequence (aa 222-237). Expression yields of a N-His_6-tagged DEP_C-$PH_{122-350}$ construct in *E. coli* are very high (20mg per L culture) and the ^{1}H,^{15}N-HSQC spectrum is indicative of a folded protein. Due to the size of the construct (229aa plus His_6-tag, 28kDa) a triple-labelled sample is required for backbone assignment. It is produced by growth in rich $^{2}H/^{15}N/^{13}C$ medium. Deuteration is checked in a ^{1}H 1D spectrum and is almost 95% for all non-exchangeable hydrogen atoms (Fig. 3.2).

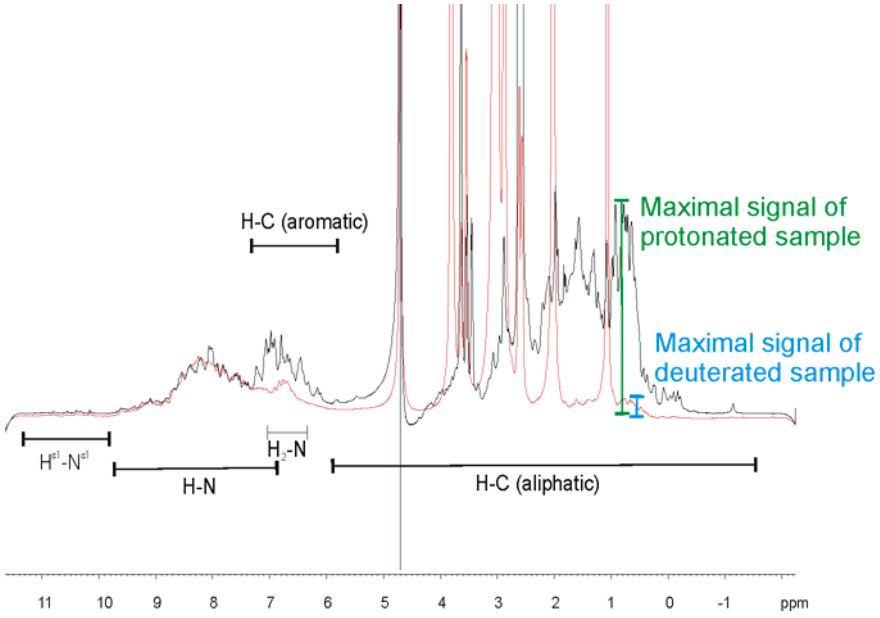

Figure 3.2: ^{1}H 1D NMR spectra of a normal (black) and a deuterated (red) sample of DEP_C-PH. *The maximal signal intensities of aliphatic carbon-bound (H-C) protons are indicated. The strong signals in the red and the black spectrum between 4 and 1ppm are from buffer components (e.g. DTT).*

3.1.2 Backbone assignment

In order to gain access to structural information backbone resonance assignment is carried out. Slowly back-exchanging amide protons of the deuterated protein resulted in around 30 (15%) weak or missing signals in triple-resonance experiments. Assignment of many of these resonances (16 H^N/N pairs and 6 H^Ns) could be achieved with a ^{15}N-HSQC-NOESY that was recorded two months after producing the sample. Since the structures of the individual domains are known, this NOESY-based H^N/N assignment of the missing residues is very reliable.

Backbone resonance assignment of the 229 amino acid protein is almost complete. The resonances of two residues of the DEP domain (Ile^{151} and Arg^{174}), of one residue of the inter-domain linker (Phe^{225}) and of five residues of C-PH (Glu^{238}, Glu^{239}, His^{256}, Arg^{257} and Arg^{258}) are absent from all spectra. There are several residues of which only the amide proton is assigned. Most of the partially or totally unassigned residues of DEP are located in the β-hairpin (aa 143-153). In the isolated DEP domain, this region is in slow

or intermediate exchange. The missing assignments of C-PH are in the β-sheet region, the N-terminal helix α1 and the β1−β2 loop. The residues of the latter are also invisible in spectra of the isolated C-PH domain, and only become structured upon ligand addition (cf. chapter 2). In total almost 90% of all backbone resonances and 93% (207/221) of all backbone (H^N,N) amide pairs are assigned. Table 3.1 summarises the statistics of the assignment.

Table 3.1: Statistics of DEP C-PH backbone assignment

	$DEP_{122-221}$	$Linker_{222-237}$	$C\text{-}PH_{238-350}$	*Total*
Assigned [1]	86	15	98	199
H^N, N only [2]	10	0	6	16
H^N only [2]	2	0	4	6
Unassigned	2	1	5	8

[1] Sequential assignment based on triple-resonance experiments and ^{15}N-NOESY.

[2] Assignments based on ^{15}N-NOESY alone.

The secondary carbon chemical shifts are shown in Fig. 3.3A. Values of δΔCA and δΔCB are calculated as the difference between measured and average/random coil CA and CB chemical shifts. δΔ(CA-CB) is strongly positive for α–helical regions and strongly negative for β-strand (extended) regions (Wishart and Sykes, 1994). refM1 Spera & Bax.

The expected secondary structure elements of DEP and C-PH are present in the double-domain construct. There is no clear indication of secondary structure in the linker region. The central linker residues Ser^{230}-Asp^{234} give rise to very strong signals in all NMR spectra and have ΔCA-ΔCB values that are typical for random coil conformation (i.e. close to zero). In particular, the triple-aspartate stretch ($Asp^{232-234}$) has completely redundant chemical shifts, reminiscent of an unfolded peptide. The linker residues that are closer to the domains have a different appearance. They have weaker signals and secondary carbon chemical shift values consistent with an extended conformation (negative ΔCA-ΔCB), in particular Cys^{226}-Gln^{229}.

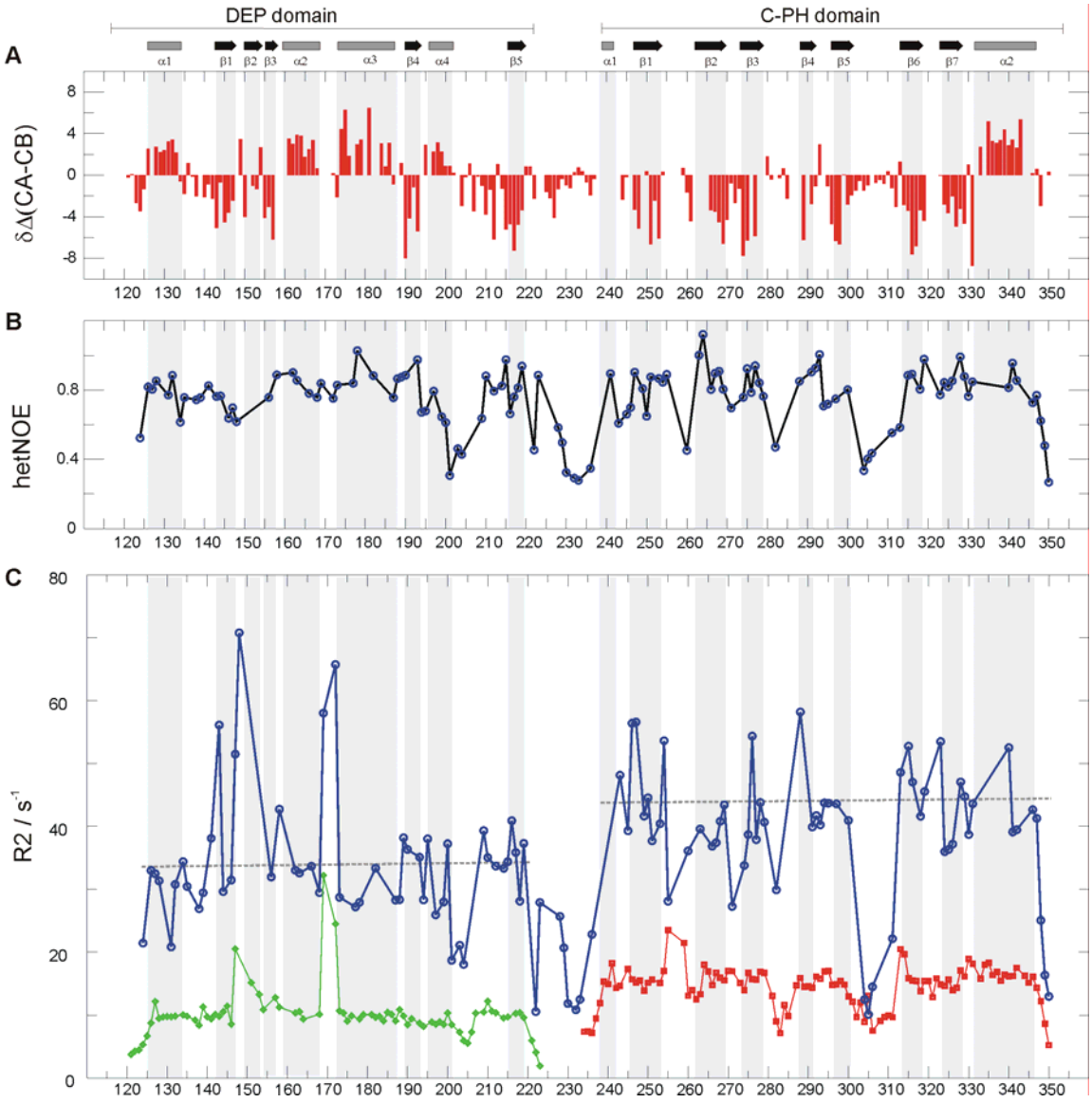

Figure 3.3: Secondary carbon chemical shifts and relaxation parameters of DEP_C-PH. *The secondary structure elements of DEP and C-PH are shaded in grey.* ***A****: Secondary carbon chemical shifts (ΔCA-ΔCB). The values are calculated as deviation from random coil chemical shifts.* ***B****: {^{1}H}-^{15}N heteronuclear NOE.* ***C****: R2 (transverse relaxation rate) of DEP_C-PH (blue), DEP (green) and C-PH (red). The average R2 value of C-PH and DEP in DEP_C-PH is indicated as a broken line.*

3.1.3 Relaxation

^{15}N NMR relaxation experiments afford insight into the dynamics of a protein's backbone chain. R1, R2 and heteronuclear NOE experiments of triple-labelled DEP_C-PH are

recorded on an 800 MHz spectrometer at 22°C. The heteronuclear NOE and R2 experiments could be analysed readily; conversely, the R1 data cannot be fitted to a single exponential decay function. This problem is unlikely to arise from experimental errors and the sample shows no sign of deterioration. Rather, the R1 experiment seems to be affected by dynamical processes that are not picked up in the other experiments or in R1 experiments of smaller proteins. Probably this is the case because the R1 curve is sampled for a very long time period (up to 2.8s) due to the size of DEP_C-PH, whereby slow or otherwise negligible dynamical processes (e.g. chemical exchange of amide protons with the solvent, multiple correlation times) become relevant. This effect is still under investigation.

The heteronuclear NOE and R2 values of DEP_C-PH are presented in Fig. 3.3B and 3.3C. For comparison, the R2 values of the single C-PH and DEP domains (both recorded at 500MHz and 22 °C) are also shown in Fig. 3.3C. Although the rates are not strictly comparable because of the difference in field strength (500 versus 800MHz) it can be clearly stated that the average R2 of DEP_C-PH is much bigger than of the single domains, as to be expected for a larger protein. However, the trend of the R2 values is very similar in the double-domain and single domain constructs. The same is true for the heteronuclear NOE values (Fig. 3.3B, data for the single domains not shown).

Remarkably, the average R2 value of DEP (~37Hz) seems to be slightly lower than of C-PH (~42Hz) in the double-domain construct (broken lines in Fig. 3.3C). This indicates that the two domains have two different correlation times and hence tumble independently in solution, although they are connected by the linker. The single isolated DEP and C-PH domains have an average R2 of 10Hz and 16Hz, respectively (at 500MHz and 295K). This dramatic difference between two domains of roughly equal size reflects that C-PH is partially dimerising/aggregating (Chapter 2), as do many other PH domains (Fushman et al., 1997; Gryk et al., 1998). The fact that the difference in average R2 is still present in DEP_C-PH indicates that there is still partial unspecific dimerisation of C-PH in DEP_C-PH, though to a lesser extent than for isolated C-PH. In fact, the sample of DEP_C-PH has no tendency to aggregate at high protein concentrations (0.5mM), while C-PH in the ligand-free state does.

^{15}N relaxation rates (R1, R2, heteronuclear NOE) are sensitive to backbone motions on a sub-nanosecond to nanosecond time-scale and. R2 values can also detect much slower motions (Palmer, 1997). In the DEP domain of DEP_C-PH, there are four regions with relaxation parameters that are indicative of differential backbone dynamics: a) the β-hairpin (aa 143-155); it has high R2 values consistent with slow dynamics, b) the turn between helices α2 and α3; also with high R2 values and presumably slow dynamics, c) helix α4 with markedly reduced heteronuclear NOE, indicating that is less rigid than the other secondary structure elements, and d) the first half of the longest loop of the DEP domain between α4 and β5 with both low NOE and R2 values, indicative of increased flexibility. All of these regions exhibit a similar profile in single DEP, with one important difference: for isolated DEP, the R2 values of the β1−β2 hairpin are notably elevated compared to the rest of the domain, but lower than those of the α2−α3 turn. In DEP_C-PH, there are more residues with elevated R2 values in or close to the β1−β2 hairpin, and the values are higher than in the α2−α3 turn. If one assumes that the dynamics of the α2−α3 turn are unchanged in DEP_C-PH compared to single DEP (which is supported by chemical shift data, see below) then the β1−β2 hairpin in DEP_C-PH experiences even more slow dynamics than in single DEP.

The inter-domain linker region is characterised by mostly low NOE and R2 values, consistent with high flexibility. Only Gly^{223} has a higher R2 and NOE. Since values for the following residues (Phe^{224}, Phe^{225}, Cys^{226} and Asn^{227}) are not available, it cannot be deduced whether Gly^{223} is an outlier or the beginning of a more structured element. C-PH displays only one region with increased backbone dynamics: the β5−β6 loop that has the hallmarks of flexibility (low R2 and NOE), just as in single C-PH. There are also two regions associated with dynamics on slow or intermediate time-scales in single C-PH, helix α1 and the β1−β2 loop. Both regions are not assigned in the double-domain construct, probably owing to just these dynamical processes. Thus, the dynamical properties of C-PH seem to be conserved in the double-domain construct.

3.1.4 Chemical shift comparison with the isolated DEP and C-PH domains

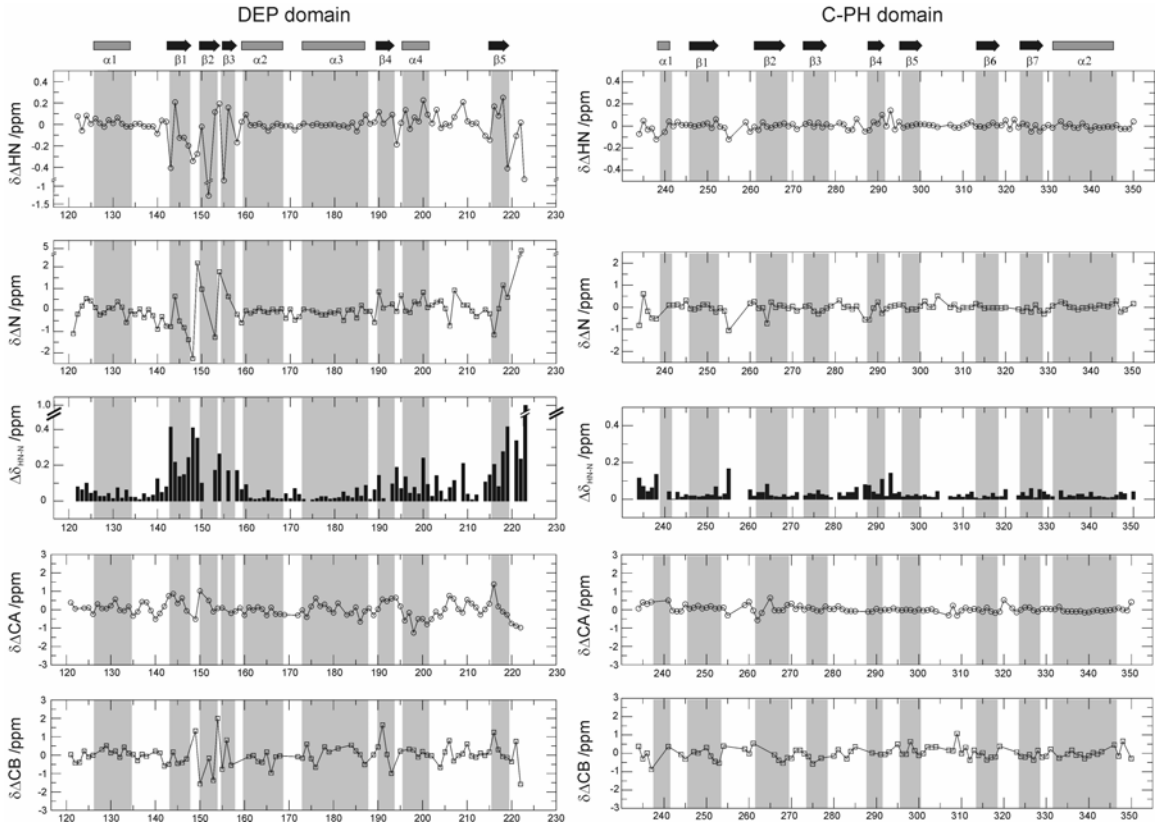

Figure 3.4: Chemical shifts differences between DEP_C-PH and the single DEP and C-PH domains. *Left column: comparison with DEP domain chemical shifts. Right column: comparison with C-PH domain chemical shifts. Chemical shift differences of H^N, N, combined H^N and N, CA and CB are shown. The secondary structure elements of DEP and C-PH are shaded in grey.*

Chemical shift is a sensitive probe of local environment. It can be employed to investigate intermolecular interactions (cf. Chapter 2), but also intramolecular ones. If two domains in a double-domain construct interact it is expected that the chemical shift of residues near the domain-domain interface will change compared to the isolated single domains.

All available H^N, N, CA and CB chemical shifts of DEP_C-PH are compared with the chemical shifts of the isolated domains so as to identify parts of the molecule that are structurally changed in the double-domain construct. The results are presented in Fig. 3.4. Surprisingly, there are large changes on the DEP domain, but only minor ones on C-PH. The region of the DEP domain that differs most strongly consists of the β1−β2 hairpin

and the β3−β5−β4 sheet. Helix α4 and the loop regions around these elements are also affected, but to a lesser degree. By contrast, the chemical shifts of the three-helix bundle (α1, α2 and α3) of DEP do not exhibit large changes. The same is true for the entire C-PH domain. Therefore it is unlikely that C-PH causes the changes on the DEP domain. In fact, the chemical shifts of the DEP domain are already affected when its C-terminus is extended into the DEP_C-PH linker up to residue 229 - without the presence of C-PH (M. Macias, unpublished results). In the $DEP_{122-229}$ construct, the additional residues 222-229 are unfolded. In DEP_C-PH, amino acids 222-229 are probably also unstructured as judged from secondary chemical shift analysis; unfortunately, no relaxation data are available for residues 224-228. The best way to explain the influence of these residues on the core DEP structure is that they associate very weakly and transiently with the DEP domain without becoming folded themselves. The strong increase in R2 values of the β1−β2 hairpin of DEP_C-PH is consistent with being involved in such a dynamic interaction.

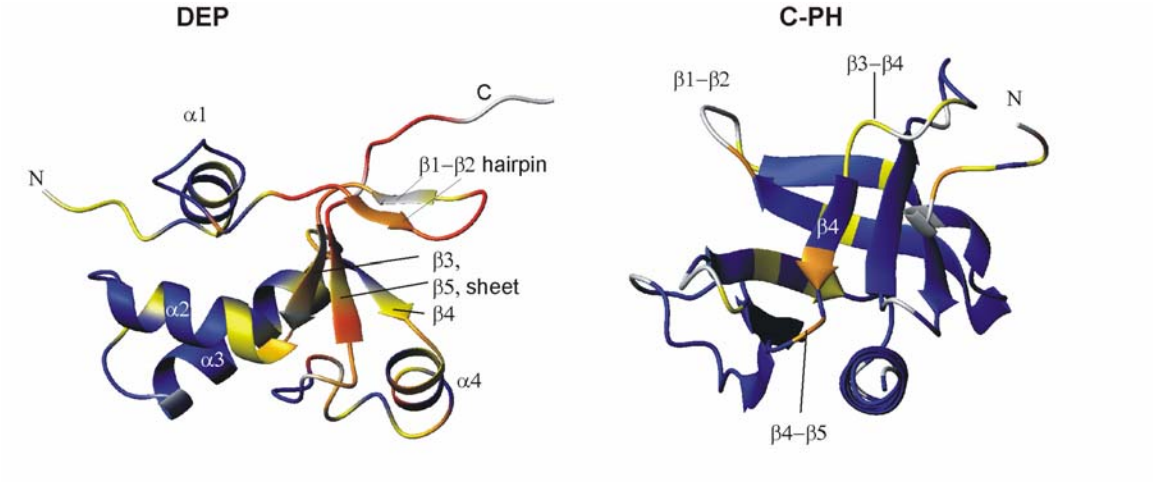

Figure 3.5: Backbone amide chemical shift differences ($\Delta\delta_{HN-N}$) mapped onto the domain structures of DEP and C-PH. *Residues are colour coded according to $\delta\Delta_{HN-N}$: no change ($\delta\Delta_{HN-N}$ <0.05) blue, small change (0.05< $\delta\Delta_{HN-N}$ <0.1) yellow, medium change (0.1< $\delta\Delta_{HN-N}$ <0.15) orange, large changes (0.15< $\delta\Delta_{HN-N}$ <0.2) dark orange, and very large changes ($\delta\Delta_{HN-N}$ >0.2) red. Grey: no data available.*

The above hypothesis is supported by inspection of the affected areas of both domains in the 3D-structures. When the combined chemical shift differences of H^N and N ($\Delta\delta_{HN-N}$)

are colour coded and mapped onto the structures of DEP and C-PH, the affected regions are highlighted (Fig. 3.5). Clearly, the whole β-region of DEP experiences strong changes in the double-domain construct. Since the C-terminus of DEP and the inter-domain linker are located in spatial proximity it is conceivable that it could fold back onto the β1–β2 hairpin. In particular, the two phenylalanine residues (Phe^{224}, Phe^{225}) at the beginning of the inter-domain linker may be involved as their aromatic rings could cause the observed large changes in chemical shift.

As for C-PH, only few and mildly effected residues are observed that are scattered all over the domain. They are preferentially located on loops and unstructured areas (N-terminus, β1–β2 loop, β3–β4 loop, β4–β5 loop), with the exception of His^{291} on the β4 strand.

3.1.5 Protein lipid overlay assay

Protein lipid overlay assays are a standard procedure to test a protein's ability to interact with phospholipids. C-PH binds specifically PtdIns(3,4)P_2 (cf. Chapter 2); therefore protein lipid overlay assays are used to test whether C-PH has the same properties in the double-domain construct and in the full-length molecule. The latter contains additionally the N-terminal PH domain (N-PH) which also binds phosphoinositides (Harlan et al., 1994; Harlan et al., 1995). N-PH, N-PH_DEP, DEP, C-PH, DEP_C-PH and full-length pleckstrin (FLP) are all expressed and purified as GST fusion proteins and used in protein lipid overlay assays, so as to characterise the lipid binding properties of all domains and domain combinations. The results of single and double-domain constructs are shown in Fig.3.6.

N-PH has a very broad spectrum of phosphoinositides it can bind to (Fig. 3.6B), including the C-PH specific PtdIns(3,4)P_2 . N-PH-DEP constructs have the same pattern as N-PH alone (panel C and D). Similarly, DEP_C-PH has the same phosphoinositide binding properties as C-PH alone (panel E and F, respectively). Note that the intensity of the PtdIns(3,4)P_2 spot for C-PH and DEP_C-PH is one order of magnitude higher than of any spot for N-PH or N-PH_DEP. As expected, the DEP domain does not bind to any lipid of the assay on its own (data not shown). Based on these binding data, it appears

that the binding site on C-PH for PtdIns(3,4)P_2 is neither obstructed nor regulated by the DEP domain in DEP_C-PH.

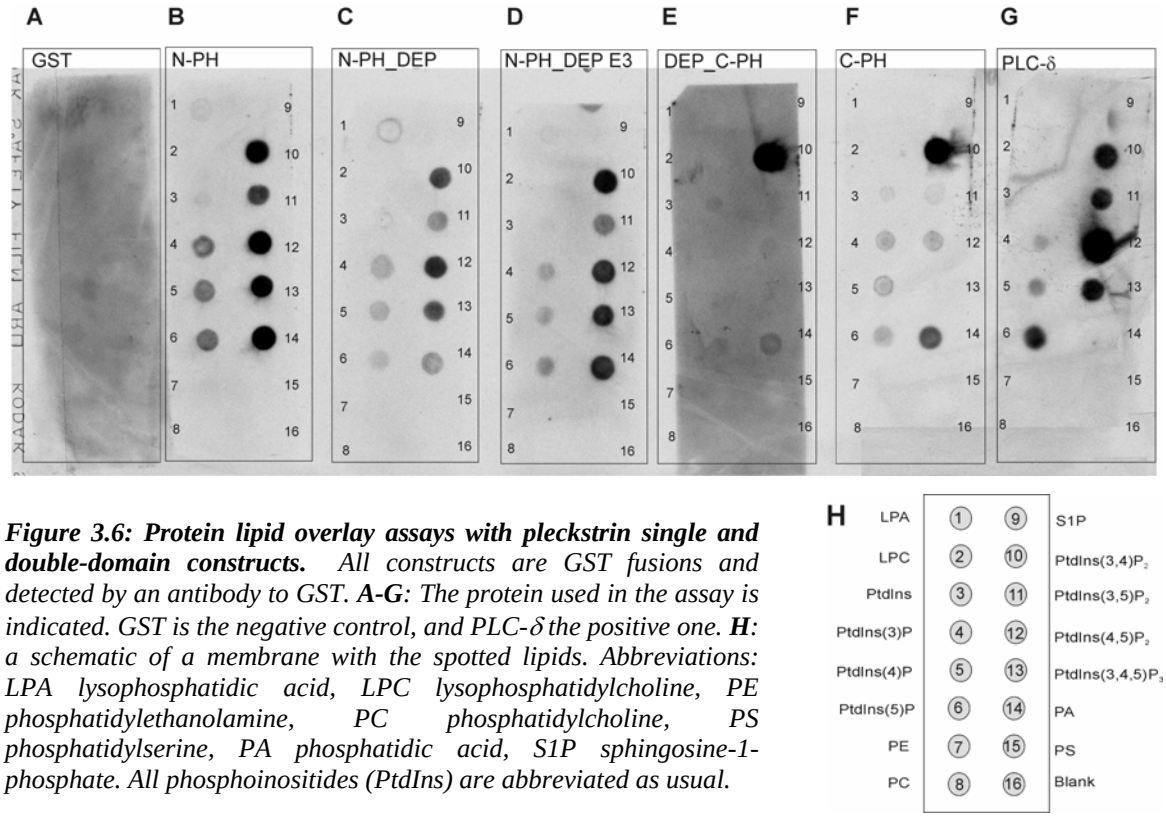

Figure 3.6: Protein lipid overlay assays with pleckstrin single and double-domain constructs. *All constructs are GST fusions and detected by an antibody to GST.* ***A-G****: The protein used in the assay is indicated. GST is the negative control, and PLC-δ the positive one.* ***H****: a schematic of a membrane with the spotted lipids. Abbreviations: LPA lysophosphatidic acid, LPC lysophosphatidylcholine, PE phosphatidylethanolamine, PC phosphatidylcholine, PS phosphatidylserine, PA phosphatidic acid, S1P sphingosine-1-phosphate. All phosphoinositides (PtdIns) are abbreviated as usual.*

Full-length pleckstrin (FLP) produces many positive signals in the lipid overlay assay (Fig. 3.7C, left), similar to N-PH (Fig. 3.6B) and N-PH_DEP (Fig. 3.6C). Unfortunately, the presence of N-PH precludes detailed analysis of the lipid binding properties of C-PH in FLP. Merely the high intensity of the PtdIns(3,4)P_2 spot, which is typical for C-PH but not for N-PH, advocates that C-PH is accessible in FLP.

Only small amounts of GST full-length pleckstrin fusion protein (GST-FLP) can be purified under standard conditions. Purification yields are increased more than tenfold when PBS with 500 instead of 150mM NaCl is used as lysis, column and wash buffer. The salt effect may arise from de-aggregation of GST-FLP, whereby the GST dimer is enabled to bind to the column. In order to investigate whether high salt also affects the binding of pleckstrin to phospholipids, the protein lipid overlay assays are repeated with

200-500mM NaCl in all (blocking, incubation, wash) buffers. The results are shown in Fig. 3.7: the overlaid pattern of N-PH and C-PH in full-length pleckstrin (panel C) is reduced to only two major spots: PtdIns(3,4)P_2 and PtdIns. The former is much more intense than the latter, and both can be safely attributed to C-PH (which on self-spotted strips also binds PtdIns, data not shown). The transition of FLP lipid binding comes about between 200 and 300mM NaCl, while 200mM NaCl already abolishes phosphoinositide binding by N-PH_DEP (panel A). Therefore, N-PH phosphoinositide binding is effectively inhibited at higher salt concentrations while C-PH retains its ability to bind to PtdIns(3,4)P_2 .

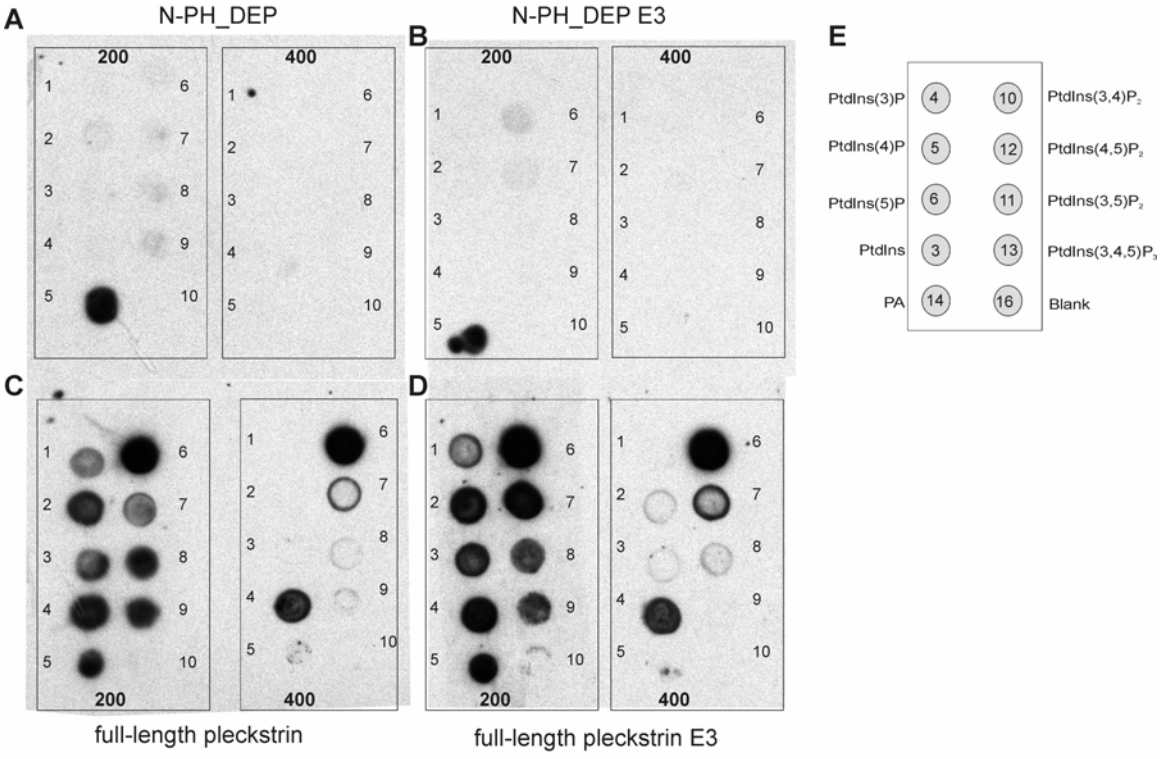

Figure 3.7: Protein lipid overlay assays in high and low salt buffers. *All constructs are GST fusions and detected by an antibody to GST.* ***A-D****: The protein used in the assay is indicated. The left and right strips of each panel are from experiments that are carried out with buffers containing 200mM NaCl and 400mM NaCl, respectively. The position of lipids on the membrane is shown in panel* ***E****. The lipid strips are self-spotted with the same concentrations as for Fig. 3.5. Abbreviations and numbering are also the same as for Fig. 3.5.*

The experiments are also carried out with the pseudo-phosphorylated variants of N-PH_DEP and full-length pleckstrin, where all three PKC acceptor sites (“S T S” in Fig.

3.1.A) are replaced with glutamate - hence the naming “E3”. The pseudo-phosphorylated variants of N-PH_DEP and full-length pleckstrin behave the same way as the wildtype (Fig. 3.7, panel B and D). Thus, neither the DEP domain, nor N-PH, nor (pseudo)phosphorylation seem to influence binding of PtdIns(3,4)P_2 by C-PH. This means that C-PH may function as an independent PtdIns(3,4)P_2 binding module.

3.2 Discussion

Several NMR studies of double-domain constructs have been previously conducted. Based on their results, one may separate two-domain proteins into three distinct groups (Fig 3.8): (A) two domains that are part of a fixed structure. (B) two domains that are connected by a short linker (3-6 residues) where the orientation between the domains is fixed or strongly restricted. (C) two domains that are independent of each other due to a long flexible linker.

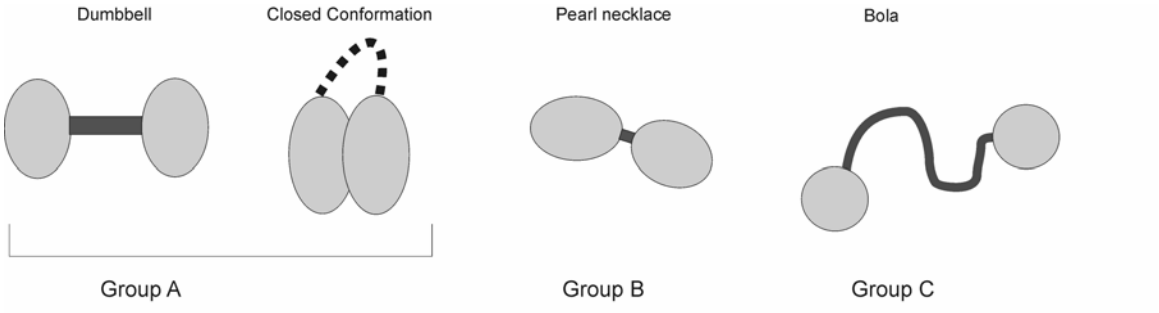

Figure 3.8: Models of double-domain arrangements. *In the dumbbell model, the domains are connected by a stiff linker. In the “closed conformation” model, both domains come in close contact. Two variants of the “beads on a string model” are shown: the “pearl necklace” model, where the spacing between the pearls restricts their movement and the “bola” model where the domains are independent.*

Two domains may form a rigid structure (group A) either because the linker between the domains is completely inflexible or because the two domains have a “closed” conformation with a large domain-domain interface. An example for the former is the structure of the Prp40 tandem WW domains, where the linker folds into a stiff helix (Wiesner et al., 2002). The “closed” conformation is observed for ubiquitin chains linked via Lys^{48} (Varadan et al., 2002). Whereas the “fixed linker” or “dumbbell” structure is

characterised by the absence of NOEs between the domains, many short distance restraints can be obtained for a "closed conformation" protein. Similarly, it is only in the closed conformation scenario that the chemical shifts of one domain are influenced by the other. What allows the closed conformation and the rigid linker structures to be grouped together is that in both cases the two domains behave as parts of a single protein. In particular RDCs and relaxation properties of the domains are governed by the same global parameters (alignment tensor, correlation time, diffusion tensor).

Group B double-domains are characterised by little or no chemical shift differences between the double-domain construct and isolated domains, with the exception of the residues closest to the linker. In some cases, a few inter-domain NOEs can be assigned, which is not sufficient to completely restrain the orientation of the two domains. However, relaxation and RDC analysis demonstrate that the orientation of the two domains is quite well defined in solution (Fushman et al., 1999; Varadan et al., 2004). The most frequently given interpretation is that the shortness of the linker and the resulting proximity of the domains are sufficient to restrict the motions of the domains relative to each other (Improta et al., 1998; Spitzfaden et al., 1997). The linker residues have relaxation parameters that are distinct from flexible loops or termini (Copie et al., 1998; Improta et al., 1998; Spitzfaden et al., 1997). It is interesting to note that the majority of group B double-domain constructs that have been studied by NMR are from proteins where multiple copies of similar or identical domains (FnI, FnIII,) are present or, in the case of ubiquitin linked via Lys^{63} (Varadan et al., 2004), where a chain of linked proteins is formed. In all of these cases, the short linker ensures an elongated overall structure of the tandem domains, which may have a role for presenting accessible surfaces to ligands and, in the case of fibronectin and titin, for defining the length of a structural element.

The last group (C) are double-domain constructs that have no specific interaction with each other and where the linker is long and flexible enough to allow completely uncorrelated dynamics of the two domains (Moreau et al., 1997; Zhou et al., 1996). The linker residues are usually very hydrophilic or charged and exhibit negative or null heteronuclear NOE values, showing that they are completely flexible. The chemical shifts do not differ significantly between the double-domain and the isolated domains.

Correlation times of the individual domains in the double-domain constructs are larger than for the single domains, consistent with being part of an overall larger structure, but may be different from one another (if the size of the domains is sufficiently dissimilar). For example, in the N-terminal portion of CheA, an *E. coli* histidine autokinase consisting of two domains (P1, 130aa and P2, 75 aa) separated by a linker of 23 residues, the correlation times are 12 and 8 ns for P1 and P2, respectively, in the double-domain protein, while P1 on its own has a correlation time of 8ns at the same temperature (303K) (Moreau et al., 1997; Zhou et al., 1995; Zhou et al., 1996).

How do the data on DEP_C-PH compare to previous studies? First, relaxation data show that the central stretch of the linker (Asn^{229}-Asp^{234}) is flexible; hence the "dumbbell" model can be excluded. Second, the size of the linker (16 residues) and the flexibility of its central residues rule out the "restrained conformation" of group B. Third, the different R2 average values (and correspondingly correlation times) of DEP and C-PH in the double-domain construct and the absence of chemical shift changes on C-PH clearly rule out the "closed" conformation. On the other hand, the length and flexibility of the linker and the absence of chemical shift changes on C-PH clearly place DEP_C-PH in group C. The biochemical data showing that C-PH binds $PtdIns(3,4)_2$ equally well in DEP_C-PH as it does on its own are also in favour of this hypothesis.

A few important differences to published group C proteins are observed. One of them is the presence of hydrophobic residues in the domain-flanking regions of the linker (Phe^{224}, Phe^{225}, Val^{235}, Ile^{236} and Leu^{237}); however, none of these residues appear to be structured in DEP_C-PH. On the other hand, the heteronuclear NOE values of the published group C domains are similar to a free peptide (negative or null), while even the most flexible residues in the DEP_C-PH linker have a NOE of at least 0.35, similar to the most flexible loops of DEP and C-PH in the double-domain construct (Fig. 3.3B). Therefore it is not clear, whether the linker is as completely flexible as, for example, in CheA. Yet, the most important difference to all examples of double-domains in the literature is the chemical shift changes on DEP in DEP_C-PH. They appear to be caused by the linker rather than by C-PH since the changes are similar in a construct consisting only of DEP and half of the linker (aa 122-229). Most likely, the chemical shift changes are caused by the aromatic sidechains of Phe^{224} and Phe^{225} because aromatic ring currents strongly

influence chemical shift. The interpretation of relaxation and chemical shift data favours a model where the linker dynamically associates with the β1−β2 hairpin without becoming sufficiently stabilised itself to result in an observable structure. In fact, one may consider the part of the linker closest to DEP as an extension of the DEP domain. Then, the DEP_C-PH double-domain construct consists of two independent units, the extended DEP domain and C-PH.

At the present time it can only be speculated whether (extended) DEP and C-PH are also independent in full-length pleckstrin. Only the protein lipid overlay assay hints at the possibility that C-PH could also be a completely independent phosphoinositide binding module in the full-length molecule. Although this is in agreement with a report claiming that both full-length pleckstrin and C-PH bind to equimolar amounts of PtdIns$(3,4)_2$ in large unilamellar vesicles (Sloan et al., 2002), more detailed studies need to confirm this result.

The studies of the DEP_C-PH double domain construct provide strong evidence that there is no close association or specific interaction between DEP and C-PH. The double-domain construct behaves much like two beads connected by a flexible string, although parts of the linker seem to associate transiently with the DEP domain. The next step to characterise the pleckstrin molecule is to analyse domain-domain interactions in triple-domain constructs. In this respect, the analysis of the double-domain constructs constitutes an important intermediate step in characterising the multi-domain protein pleckstrin and provides a basis to tackle the more technically demanding, but also biologically more interesting, full-length protein.

3.3 References

Copie, V., Tomita, Y., Akiyama, S. K., Aota, S., Yamada, K. M., Venable, R. M., Pastor, R. W., Krueger, S., and Torchia, D. A. (1998). Solution structure and dynamics of linked cell attachment modules of mouse fibronectin containing the RGD and synergy regions: comparison with the human fibronectin crystal structure. J Mol Biol *277*, 663-682.

Fushman, D., Cahill, S., and Cowburn, D. (1997). The main-chain dynamics of the dynamin pleckstrin homology (PH) domain in solution: analysis of 15N relaxation with monomer/dimer equilibration. J Mol Biol *266*, 173-194.

Fushman, D., Xu, R., and Cowburn, D. (1999). Direct determination of changes of interdomain orientation on ligation: use of the orientational dependence of 15N NMR relaxation in Abl SH(32). Biochemistry *38*, 10225-10230.

Gryk, M. R., Abseher, R., Simon, B., Nilges, M., and Oschkinat, H. (1998). Heteronuclear relaxation study of the PH domain of beta-spectrin: restriction of loop motions upon binding inositol trisphosphate. J Mol Biol *280*, 879-896.

Harlan, J. E., Hajduk, P. J., Yoon, H. S., and Fesik, S. W. (1994). Pleckstrin homology domains bind to phosphatidylinositol-4,5-bisphosphate. Nature *371*, 168-170.

Harlan, J. E., Yoon, H. S., Hajduk, P. J., and Fesik, S. W. (1995). Structural characterization of the interaction between a pleckstrin homology domain and phosphatidylinositol 4,5-bisphosphate. Biochemistry *34*, 9859-9864.

Improta, S., Krueger, J. K., Gautel, M., Atkinson, R. A., Lefevre, J. F., Moulton, S., Trewhella, J., and Pastore, A. (1998). The assembly of immunoglobulin-like modules in titin: implications for muscle elasticity. J Mol Biol *284*, 761-777.

Moreau, M., de Cock, E., Fortier, P. L., Garcia, C., Albaret, C., Blanquet, S., Lallemand, J. Y., and Dardel, F. (1997). Heteronuclear NMR studies of E. coli translation initiation factor IF3. Evidence that the inter-domain region is disordered in solution. J Mol Biol *266*, 15-22.

Palmer, A. G., 3rd (1997). Probing molecular motion by NMR. Curr Opin Struct Biol *7*, 732-737.

Sloan, D. C., Wang, P., Bao, X., and Haslam, R. J. (2002). Translocation of pleckstrin requires its phosphorylation and newly formed ligands. Biochem Biophys Res Commun *293*, 640-646.

Spitzfaden, C., Grant, R. P., Mardon, H. J., and Campbell, I. D. (1997). Module-module interactions in the cell binding region of fibronectin: stability, flexibility and specificity. J Mol Biol *265*, 565-579.

Varadan, R., Assfalg, M., Haririnia, A., Raasi, S., Pickart, C., and Fushman, D. (2004). Solution conformation of Lys63-linked di-ubiquitin chain provides clues to functional diversity of polyubiquitin signaling. J Biol Chem *279*, 7055-7063.

Varadan, R., Walker, O., Pickart, C., and Fushman, D. (2002). Structural properties of polyubiquitin chains in solution. J Mol Biol *324*, 637-647.

Wiesner, S., Stier, G., Sattler, M., and Macias, M. J. (2002). Solution structure and ligand recognition of the WW domain pair of the yeast splicing factor Prp40. J Mol Biol *324*, 807-822.

Wishart, D. S., and Sykes, B. D. (1994). Chemical shifts as a tool for structure determination. Methods Enzymol *239*, 363-392.

Zhou, H., Lowry, D. F., Swanson, R. V., Simon, M. I., and Dahlquist, F. W. (1995). NMR studies of the phosphotransfer domain of the histidine kinase CheA from Escherichia coli: assignments, secondary structure, general fold, and backbone dynamics. Biochemistry *34*, 13858-13870.

Zhou, H., McEvoy, M. M., Lowry, D. F., Swanson, R. V., Simon, M. I., and Dahlquist, F. W. (1996). Phosphotransfer and CheY-binding domains of the histidine autokinase CheA are joined by a flexible linker. Biochemistry *35*, 433-443.